Heliyon 10 (2024) e23849

Contents lists available at ScienceDirect

Heliyon

journal homepage: www.cell.com/heliyon

Antibacterial evaluation of different prosthetic liner textiles coated by CuO nanoparticles

Ziba Najmi [a,1], Nives Matijaković Mlinarić [b,1], Alessandro Calogero Scalia [a], Andrea Cochis [a], Atiđa Selmani [c], Aleksander Učakar [d], Anže Abram [d], Anamarija Zore [b], Ida Delač [e], Ivan Jerman [f], Nigel Van de Velde [f], Janja Vidmar [g], Klemen Bohinc [b,**], Lia Rimondini [a,*]

[a] *Department of Health Sciences, Center for Translational Research on Autoimmune and Allergic Diseases-CAAD, Università Del Piemonte Orientale UPO, Corso Trieste 15/A, 28100, Novara, NO, Italy*
[b] *University of Ljubljana, Zdravstvena Pot, 1000, Ljubljana, Slovenia*
[c] *Pharmaceutical Technology and Biopharmacy, Institute of Pharmaceutical Sciences, University of Graz, Universitätsplatz 1, 8010, Graz, Austria*
[d] *Institut Jožef Stefan, Jamova Cesta 39, 1000, Ljubljana, Slovenia*
[e] *Institute of Physics, Bijenička Cesta 46, 10000, Zagreb, Croatia*
[f] *National Institute of Chemistry, Hajdrihova Ulica 19, 1000, Ljubljana, Slovenia*
[g] *Department of Environmental Sciences, Jožef Stefan Institute, Jamova Cesta 39, 1000, Ljubljana, Slovenia*

ARTICLE INFO

Keywords:
Prosthetic liner
Textile
Copper
Nanoparticle
Antibacterial
Cytocompatibility

ABSTRACT

Prosthetic liners are mainly used as an interface between residual limbs and prosthetic sockets to minimize physical and biological damage to soft tissue. However, the closed and moist conditions within liners and the amputee's skin provide a suitable environment for bacterial growth to cause infections. This study aimed to coat a comprehensive variant material with copper oxide nanoparticles (CuO NPs) and compare their surface analysis and antibacterial properties. These materials were covered with CuO NPs solution at a concentration of 70 μg mL^{-1} to achieve this purpose. After drying, their surface characteristics were analyzed by measuring zeta potential, contact angle, surface roughness, and fiber arrangement. Cu-released concentration from the coatings into the acetate buffer solution by inductively coupled plasma mass spectrometry indicated that lycra and nylon quickly released Cu ions to concentrations up to ~0.2 μg mL^{-1} after 24 h, causing low metabolic activity of human bone–marrow mesenchymal stem cells (bMSC) in the indirect assay. Antibacterial activity of the coated specimens was evaluated by infecting their surfaces with the Gram-positive bacteria *Staphylococcus epidermidis,* reporting a significant ~40 % reduction of metabolic activity for x-dry after 24 h; in addition, the number of viable bacterial colonies adhered to the surface of this material was reduced by ~23 times in comparison with non-treated x-dry that were visually confirmed by scanning electron microscope. In conclusion, CuO NPs x-dry shows optimistic results to pursue further experiments due to its slow speed of Cu release and prolonged antibacterial activity, as well as its compatibility with human cells.

* Corresponding author.
** Corresponding author.
E-mail addresses: klemen.bohinc@zf.uni-lj.si (K. Bohinc), lia.rimondini@med.uniupo.it (L. Rimondini).
[1] These authors have contributed equally to this work.

https://doi.org/10.1016/j.heliyon.2023.e23849
Received 17 July 2023; Received in revised form 3 December 2023; Accepted 13 December 2023
Available online 17 December 2023

1. Introduction

Over several decades, amputation of short and long limbs has sometimes been considered the only and inevitable solution, despite innovations in the surgical field and new diagnostic procedures for severe diseases such as vascular disease, diabetes, etc. [1]. In 2017, about 60 million people were suffering from amputation worldwide caused by falls (36.2 %), car accidents (15.7 %), and other physical injuries (10.4 %), with high occurrence in the developing countries, and this number is predicted to rise to about 200 million by the end of 2050 [2]. Residual limb soft tissues are not accustomed to tolerating pressure and loads, and being in contact with the prosthetic socket for a long time can cause ulceration on the skin; moreover, protecting the soft tissue of the lower limb amputees is still challenging [3].

Prosthetic liner, which applies as an interference part between the rigid socket and soft tissue of the residual limb, plays two pivotal roles: protection of skin from friction damages occurring in contact with the socket and coupling the residual limb to the prosthesis to have a functional application [4]. On the other hand, prosthetic liner has been referred to as 'second skin' due to its close contact with the amputee's skin, which is constantly inhabited by hundreds of different life forms, including various species of bacteria and fungi that make up the skin's microbiota [5,6]. The skin microflora interacting with the host body can protect the skin or increase its vulnerability [7]. A confined, warm, and damp condition at the prosthetic liner-skin interface supplies a suitable environment for bacterial and fungal pathogens to grow and promote irritation and local infection that might lead to an infection of the residual limb [8]. The most common microorganisms found in the skin of amputees utilizing prosthetic liners that cause cutaneous infections, abscesses, folliculitis, and scalded-skin syndrome are *Staphylococcus aureus* and *Staphylococcus epidermidis* [9,10].

Studies showed that more than 70 commercial prosthetic liners have been available on the market, demonstrating much attention to developing materials to manage temperature, perspiration, and infections [11]. Some natural (wool and silk) and synthetic (nylon, neoprene, lycra, and polypropylene) fabric materials are commonly used for prosthetic liners due to their conformability, resiliency, and perspiration [12]. Combining these materials with antibacterial agents can develop prosthetic liners with intrinsic antibacterial properties to simultaneously reduce the disturbance of prosthetic sockets and skin infections.

Recently, many researchers have been implementing nanoscale materials, such as metallic and metallic oxide nanoparticles (NPs), as substitutions for common antibiotics to reduce the number of multidrug-resistant bacteria. Because of the diverse concurrent action mechanisms of metallic nanoparticles towards pathogens, bacterial cells have difficulty developing multiple mutations to be resistant to these nanoparticles [13]. Among the metallic and metallic oxide NPs, silver (Ag) [14,15], zinc oxide (ZnO) [16], copper (Cu) [17], cupric oxide (CuO) [18], and cuprous oxide (Cu_2O) have attracted noticeable consideration due to their implementation in electronics, optical sensors, and therapeutic applications. In addition, they exhibit broad-spectrum antibacterial activity against Gram-positive (*Bacillus subtilis – B. subtilis, S. aureus*) and Gram-negative (*Pseudomonas aeruginosa – P. aueruginosa, Escherichia coli – E. coli*) bacterial strains [19].

The antibacterial properties of doped textile materials with CuO NPs can be explained through three different strategies: 1) electrostatic interaction of the released copper ions (Cu^{2+}) with some negative-charged functional groups on the cell wall or cell membrane of bacteria [20]; 2) direct effect of nanoscale CuO NPs (with dimension less than 10 nm) on bacterial cells by passing through the cell wall and entering the cytoplasm. Consequently, NPs can inhibit DNA replication or alter the helical structure by binding to DNA [21] and 3) induction of reactive oxygen species (ROS) and production of oxidative stress that can lead to lipid peroxidation and oxidation of proteins, DNA, and RNA [22].

This current study demonstrates a comprehensive research, containing surface assessment of different materials after coating with CuO NPs, cytocompatibility and antibacterial activity evaluation, and the effect of released Cu ions on human cells. Additionally, this work reports for the first–time extensive research on five different materials (natural and synthetic fibers) after being coated with CuO NPs; previous publications have focused on a specific subject with limited samples. For example, the synergistic effect of silver-carried CuO nanosheet composites for antibacterial properties towards *E. coli, P. aeruginosa,* and *S. aureus* was evaluated by Ni et al. [23]. To achieve these purposes, first, the surfaces of five different materials (lycra, neoprene, x-dry, bamboo, and nylon) were coated with CuO NPs and their physio-chemical properties were evaluated by measuring zeta potential, contact angle, surface roughness, and fiber arrangement. Then, the potency of the released ions from the coated specimens was assessed by inductively coupled plasma mass spectrometry (ICP-MS). Materials were then infected with a Gram-positive bacterial pathogen (*S. epidermidis*) to evaluate their antibacterial characterizations. Finally, the cytocompatibility activity of the doped materials was assessed towards human bone–marrow mesenchymal stem cells (bMSCs).

2. Materials and methods

2.1. Samples preparation

2.1.1. CuO nanoparticles

CuO nanoparticles (CuO NPs) were prepared using following analytical–grade chemicals (Sigma Aldrich, Burlington, USA): $CuSO_4{\cdot}5H_2O$ (0.1 mol dm^{-3}), NaOH (1 mol dm^{-3}), and sodium poly (4-styrene sulfonate), PSS (w = 0.5 %) without further purification. The stock solutions were prepared by dissolving the $CuSO_4{\cdot}5H_2O$ and NaOH in deionized water (conductivity <0.055 μs cm^{-1}). CuO was synthesized by adding 0.5 mL NaOH (c (NaOH) = 1.0 mol dm^{-3}) to a 2 mL $CuSO_4$ solution (c ($CuSO_4$) = 0.1 mol dm^{-3}). The prepared solution was heated to 60 °C and stirred magnetically (300 rpm) until the color changed from blue to black. The obtained NPs were separated from the solution by centrifugation at 6000 rpm for 10 min and washed with deionized water in several cycles. The collected material was dried at 100 °C for 5 h. The dried mass was annealed in an oven (Nabertherm, Bremen, Germany) at 400 °C for 2

h to obtain highly crystalline CuO NPs.

2.1.2. Textile

The surfaces of five different natural and synthetic materials (lycra, neoprene, nylon, bamboo fibers, and x-dry; dimension 2 × 2 cm), which validated commercial for human application for prosthetic liners and socks and provided by MOOR Ortotika (Protetika, Ljubljana, Slovenia), were cleaned by immersing in ethanol (70 % v/v), shaking for 10 min and washing several times with distilled water. A stock solution of CuO NPs with a concentration of 500 μg mL^{-1} was prepared by suspending an appropriate mass of CuO NPs in Milli-Q water under pulsed ultrasound irradiation and by adding 80 μL of PSS (w = 0.5 %) for suspension stabilization. For the further treatment of the materials, the stock solution was diluted to 70 μg mL^{-1}. Afterwards, 100 μL of this solution was added to the materials' surfaces and left to dry at 60 °C for 3 h.

2.2. CuO nanoparticle characterization

Fourier transform infrared (FTIR) spectra of CuO NPs were measured in the 400–4000 cm^{-1} range using the PerkinElmer FT-IR C89391 instrument (PerkinElmer, Massachusetts, USA). Surface characterizations of NPs were investigated by X-ray diffraction on the polycrystalline material (XRD) on the Aeris Panalytical Diffractometer (Malvern Panalytical, Malvern, United Kingdom) using Ni-filtered copper radiation in the Bragg-Brentano geometry in the 2θ-range 5 °–70° with a step size of 0.005°, 10 s per step. The CuO NP material was put on a silicon zero-background material holder. The obtained diffraction results were analyzed with PANalytical High Score Plus software.

The size of CuO NPs was measured in Milli-Q water at 25 °C by dynamic light scattering (DLS). The measurement was performed with the Litesizer 500 (Anton Paar, Graz, Austria), equipped with a 40 mW semiconductor laser diode operating at 658 nm. The measurement was repeated three times and the obtained data were analyzed using Kalliope version 1.2.0.

Finally, the morphology of NPs was visually observed by the Schottky field emission scanning electron microscope (JSM-7600 F, Jeol Ltd, Tokyo, Japan). The size of the NPs was additionally determined from the SEM images by using ImageJ software.

2.3. Surface characterization of CuO NPs–coated materials

2.3.1. Evaluation of samples' hydrophobicity

The contact angle between the surfaces of materials and the drop of water was measured using the sessile drop technique with the Attension Theta Tensiometer (Biolin Scientific AB, Gothenburg, Sweden). 5 μL of water was added like a drop, which was produced by the tip of a needle (with diameter 0.4 mm), onto the samples' surfaces and contact angle measurement was performed when three-phase boundary (samples' surface– air– water drop) was not moving.

2.3.2. Evaluation of surface charge of samples

Surface charge of the materials before and after coating with CuO NPs was performed with measurement of zeta potential by using a SurPASS electrokinetic analyzer (Anton Paar GmbH, Graz, Austria) at 19–22 °C in 1 mmol dm^{-3} potassium bromide at pH 6.5 [24].

2.3.3. Surface roughness

The surface roughness of textiles was determined by non-contact optical profilometry [25]. The surface topography of the materials was measured on the Zygo Zegage Pro optical profilometer HR (Zygo Corporation, Middlefield, CT, USA) using coherence scanning interferometry. The light from a white LED illuminator was split into two light beams. One of the light beams was directed at the textile surface and the other at the internal reference. The 3D surface on an array detector was obtained by recombining the reflections from the surface and the internal reference. Before the measurement, the textiles were coated with 5–10 nm platinum and 20 nm carbon. The morphology of the fabric was confirmed by scanning electron microscopy (SEM) equipped with TESCAN tungsten filament microscopes VEGA3 (Tescan, Brno—Kohoutovice, Czech Republic).

2.3.4. Ion release evaluation – dissolution of CuO NPs

The specimens were immersed in a 5 mL acetate buffer (pH = 5.5) for 24 h without mixing. Then, the materials were removed and the solutions were filtered through 0.22 μm pore filters; the filtrate was acidified by adding 0.34 % nitric acid (67–69 % HNO3, high purity, Carlo Erba Reagents, Italy) and mixing for 10 s with a vortex mixer (Vibromix 10, Tehtnica, Železniki, Slovenia). Afterwards, it was diluted 100-fold with Milli-Q water prior to their analysis by inductively coupled plasma mass spectrometry (Agilent 7700x ICP-MS, Agilent Technologies, Tokyo, Japan) equipped with an autosampler (ASX-500, Agilent Technologies), a Teflon Mira Mist nebulizer, and a Scott-type quartz double spray chamber. The blank acetate buffer was considered a control solution. The ICP-MS instrumental parameters optimized for best sensitivity and robustness are listed in Table S1 in the supplementary materials. Quantification of measured Cu concentration was verified by a standard curve of Cu in the range concentration of 0.1–500 μg L^{-1}. Matrix-matched calibration standards were prepared from standard solutions containing 1000 μg mL^{-1} Cu in 2–3% HNO_3 (Merck). The performance of the analytical procedure for the determination of Cu concentration was evaluated by analyzing a blank acetate buffer solution spiked with 500 μg L^{-1} Cu standard.

2.4. Biological characterisation

2.4.1. Antibacterial activity

2.4.1.1. Growth condition of bacteria. The methicillin-resistant Gram-positive *S. epidermidis* used to evaluate the antibacterial properties of CuO NPs–coated specimens was acquired from the American type culture collection (ATCC 51625, Manassas, USA). 2–3 colonies of bacteria which had grown on Trypticase soy agar (TSA, Merck, Italy) at 37 °C, were collected and resuspended in 30 mL of Luria Bertani (LB, Merck, Italy) and incubated at 37 °C, 120 rpm for overnight. A new sub-culture was prepared prior to each experiment, and the experiments were carried out with 1×10^3 CFU/mL by measuring the optical density of bacterial suspension. LB medium without infection was considered as a control.

2.4.1.2. Investigation of antibacterial activity. The textile specimens were sterilized in the autoclave condition with a temperature 121 °C for 15 min. To evaluate the direct antibacterial impact of the CuO NPs–coated specimens, needed number of bacteria (1×10^3 CFU/mL) was resuspended into 50 μL of LB culture medium and dropped directly onto the surfaces. After 24 h of incubation, the antibacterial evaluation of the materials was analyzed using metabolic activity with colorimetric/fluorometric alamar blue assay (alamarblue™ ready-to-use solution from Life Technologies). In brief, the solution of 0.0015 % alamar blue was added directly into the wells containing infected specimens and kept in the incubator for 4 h according to the manufacturer's instructions. The alamar blue reagent contains a blue and non-fluorescent component called resazurin that is metabolically reduced only by viable cells (human or bacterial cells) to a pink and fluorescent component named resorufin. Then, fluorescence intensity of the resorufin was measured using a spectrophotometer (Spark multimode microplate reader, Tecan) at an emission wavelength of 590 nm; Therefore, the number of viable cells correlates to the fluorescent intensity of the resorufin indicating as reflective fluorescent unit (RFU) value. The non-coated materials were assumed control samples with high metabolic activity (100 %) due to the fact they are validated commercial materials for liners and socks; based on these premises the results of the metabolic activity of the surface–attached bacterial cells on the CuO–coated samples were normalized with the control samples.

Viable surface-adhered bacteria were counted after 24 h using the colony–forming unit (CFU) assay. Briefly, the materials were transferred to sterile tubes containing 1 mL of PBS, and bacteria were detached from the specimens' surfaces using sonication (5 min each, 3 times) and vortex (20 s each, 3 times). Then, different serial dilutions of bacterial suspension were prepared by mixing them with PBS; 20 μL of each dilution was spotted on an agar plate and 24 h after incubation the number of CFU was calculated through this formula [26]:

$$\text{CFU: (number of colonies} \times \text{dilution factor)} \times 10^{\text{serial dilution}}$$

Finally, the morphologies of surface-adhered bacteria were visually investigated by scanning electron microscope imaging (JSM-IT500, JEOL, Japan). Accordingly, the specimens were fixed with 2.5 % glutaraldehyde, dehydrated with an alcoholic scale (70–90 % ethanol for 1 h each and 100 % for 2 h), rapidly dried with hexamethyldisilazane, and sputtered with the JEOL Smart Coater (JEOL, Japan).

2.4.2. Cytocompatibility activity

2.4.2.1. Cell growth condition. Mesenchymal stem cells isolated from human bone marrow (bMSC), which were commercially available in PromoCell (C-12974), were cultivated in Dulbecco's Modified Eagle Medium (DMEM, Sigma-Aldrich, with 1 g/L of glucose concentration) supplemented with 15 % fetal bovine serum (FBS, Sigma-Aldrich) and 1 % of antibiotic such as penicillin-streptomycin (PS, Merck, Italy) at 37 °C in a 5 % CO_2 atmosphere. When cells' growth reached until 80–90 % confluency, they were detached by a trypsin-EDTA solution (0.25 % in PBS), and used for experiments.

2.4.2.2. Investigation of cytocompatibility activity. To evaluate cytocompatibility activity in direct way, cells (1.5×10^4 cells/material) were seeded on the surfaces of materials and incubated at 37 °C for 4 h to ensure the cells adhered and spread properly onto the specimens' surfaces. Afterwards, 1 mL of DMEM medium was added and incubated at 37 °C for 24 h. The metabolic activity of the surface-adhered cells was evaluated using the colorimetric/fluorimetric assay alamar blue (as explained in Section 2.4.1.2).

According to the protocol of the International Organization of Standardization (ISO 10993–5: 2009), the indirect cytocompatibility assay was recommended for evaluation of the cytotoxicity effect of an extract that was obtained by immersing coated samples in the appropriate culture medium of a cell line. In other words, if the coated layer released from the samples into the culture medium has a cytotoxic effect, it can be evaluated by measuring the metabolic activity of the cells [27,28]. Accordingly, following the above-mentioned standard, the materials were immersed in 7 mL of cell culture medium and incubated in the agitation (120 rpm) at 37 °C for 7 days. Afterwards, this culture medium was utilized for cultivation of bMSC cells at a needed concentration (1.5×10^4 cells/material) in a 24-multiwell plate, which was incubated at 37 °C with 5 % CO_2 for 24 h. The metabolic activity of the surface-adhered cells was evaluated using the colorimetric/fluorimetric assay alamar blue (as explained in Section 2.4.1.2).

2.5. Statistical test

All biological experiments were performed in triplicate. The statistical analysis of the data were carried out by SPSS software (v.

20.0, IBM, USA). Initially, the normal distribution of the data and the homogeneity of variance were assessed by the Shapiro-Wilk's test and Levene's test, respectively. Then, the results of the treated groups were compared with the control ones by one-way comparison ANOVA and Tukey's test as a post hoc analysis. P value < 0.05, and p value < 0.01 were considered as statistical differences shown here by * and **, respectively.

3. Results

3.1. Nanoparticles characterization

CuO NPs were prepared by dissolving individual salts in deionized water and heating at high temperature; then, their morphology and characterizations were analyzed by SEM, FTIR, and X-ray diffraction, and the results are presented in Fig. 1A–C. The SEM images of the CuO NPs showed nano-sized CuO crystal flakes with irregular shapes and ragged edges (Fig. 1A). The mean particle size of the prepared CuO NPs determined by dynamic light scattering (DLS) was 778 ± 62 nm, which was consistent with the SEM images. In addition, the thickness of the nanoflakes was determined using ImageJ software (d = 50.5 ± 13.5 nm). The morphological features were attributed to crystal growth in the [100] and [010] directions under Ostwald ripening [29]. The FTIR spectrum of the material shows the presence of characteristic metal oxide groups (Fig. 1B). The observed peaks at specific wavenumbers (ν/cm^{-1}) correspond to symmetric Cu–O stretching (404 cm^{-1}), asymmetric Cu–O stretching (483 cm^{-1}) and Cu–O wagging (610 cm^{-1}). The vibration peak at 3572 cm^{-1} in the material dried at 100 °C indicates the presence of hydroxide groups (O–H stretching) left after washing the material with NaOH. These molecules are no longer present after annealing, indicating that the CuO material is pure and suitable for further applications. The formation of CuO NPs from copper sulfate is indicated by metal-oxygen bonds at 1641 cm^{-1} (Cu–O rocking out-of-plane) and 1350 cm^{-1} (Cu–O rocking in-plane) [30]. The structural and chemical compositions were additionally confirmed by X-ray diffraction on the polycrystalline CuO material (Fig. 1C). Based on the Joint Committee on Powder Diffraction Standards (JCPDS card No. 80–1917), the XRD pattern corresponds to the monoclinic CuO phase. The material after annealing showed more pronounced intensities and narrower peaks (002 and 111), indicating better crystallinity than the dried material. Due to their higher purity and crystallinity, the annealed CuO NPs were added to the selected textile materials.

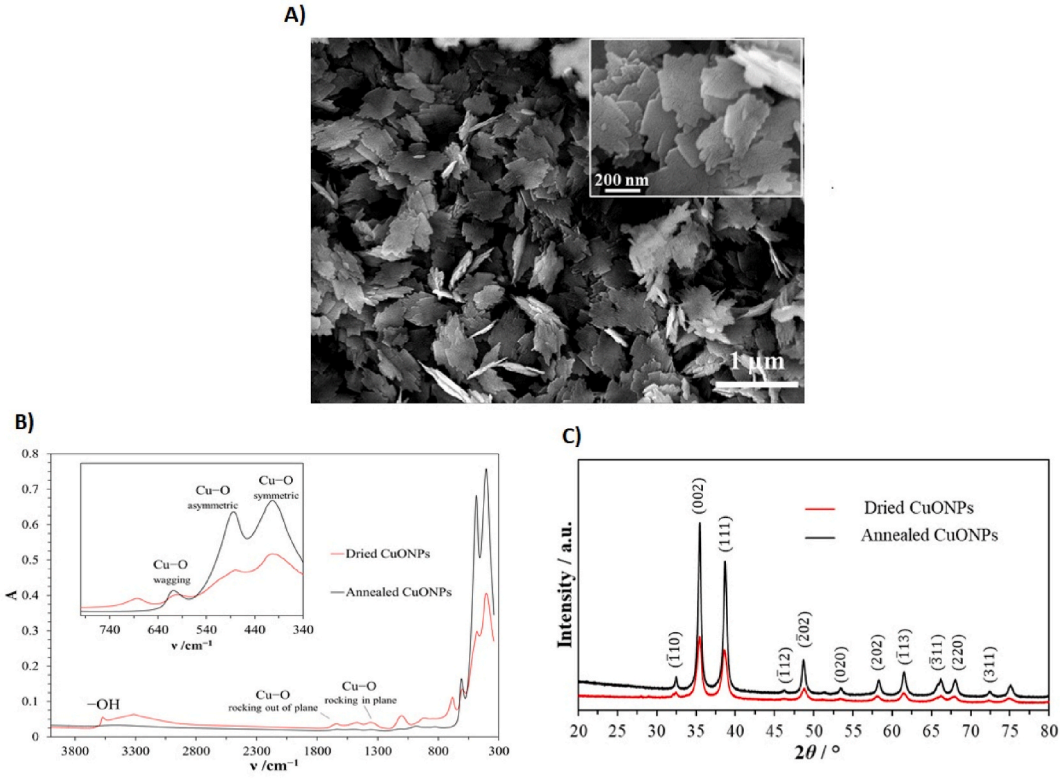

Fig. 1. CuO NPs characterization: A) SEM images of CuO NPs; B) FTIR spectra of CuO NP material dried at 100 °C (red line) and annealed at 400 °C (black line), A and ν indicate absorbance and wavenumbers, respectively; C) X-ray diffractogram of CuO NP material dried at 100 °C (red line) and annealed at 400 °C (black line).

3.2. Material surfaces' characterization after coating by CuO NPs

The zeta potential of CuO NPs–coated materials (lycra, nylon, neoprene, bamboo fibers, and x-dry) is shown in Fig. 2A; non-treated materials were considered control materials. The positive charge of the surfaces promotes the adhesion of negatively charged bacteria through electrostatic interactions, and vice versa [31]. The results showed a negative surface zeta potential for all tested materials. Prior to coating the materials with CuO NPs, neoprene had the highest negative potential, followed by x-dry, lycra, and nylon, while bamboo fibers had the smallest negative zeta potential. The zeta potential measurement of coated specimens revealed a decrease in negative charge for bamboo fibers ($\zeta = -97 \pm 2$ mV), nylon ($\zeta = -139 \pm 3$ mV), lycra ($\zeta = -148 \pm 3$ mV), and x-dry ($\zeta = -262 \pm 10$ mV). However, coated neoprene showed an increase in zeta potential up to -246 ± 2 mV. The highest negative surface potential after treatment with CuO NPs was observed for the x-dry material.

The hydrophobicity of the materials' surfaces before and after coating was determined by measuring the static water contact angle (CA). As shown in Fig. 2B, no significant differences were observed between CuO NPs–coated materials and non-treated specimens that were considered control materials. Among these materials, nylon, neoprene, and x-dry revealed intrinsic hydrophobicity properties with contact angles of 115.78° ± 1.37°, 126.85° ± 6.95°, and 98.02° ± 8.12° respectively.

The 2D surface profile of the specimens was measured using optical profilometry, indicating that lycra contained smaller fiber bundles with smaller height differences between the upper and lower bundles (Fig. S1 in the supplementary materials). To confirm the optical profilometry observations, pristine lycra textilee were also selected for in-depth analysis by SEM. The material was interwoven with fibers that were ~10 μm in diameter (Fig. S2 A-C in the supplementary materials indicates SEM images of non-coated lycra at different magnifications); after coating the materials with CuO NPs, some sporadic nanoflakes demonstrating NPs on the fibers' surfaces were detected by using SEM (Fig. S2 D in the supplementary materials shows the SEM images of CuO NPs–coated lycra as a representative material). The results obtained from optical profilometry were confirmed by SEM images, indicating a variation in fiber arrangement within the tested specimens; for example, the bamboo fibers were arranged in large spiral fiber bundles with loose fibers on the material's surface. The neoprene material contained loosely packed fibers with low fiber alignment. The nylon material showed a random arrangement of fibers with no ordered structure and significant differences in height between the fibers. The x-dry material showed densely packed fiber bundles with large height differences between the individual bundles. The surface roughness of the specimens indicated as root mean square (RMS) was determined between 29 and 154 μm, with the lowest surface roughness found in the materials made of lycra and nylon and the highest in the material with bamboo fibers (Fig. 2C).

To evaluate the capacity of specimen ion release, the materials were submerged in 5 mL of acetate buffer with pH 5.5, the optimum pH of the skin, and incubated for 24 h; afterwards, the materials were removed and cultured media containing released ions was diluted 100 times in Milli-Q water. The concentration of released ions was measured using ICP-MS, and the results in Fig. 2D show that lycra and nylon released Cu up to about 0.2 μg mL^{-1} after 24 h, whereas the other specimens (neoprene, x-dry, and bamboo fiber)

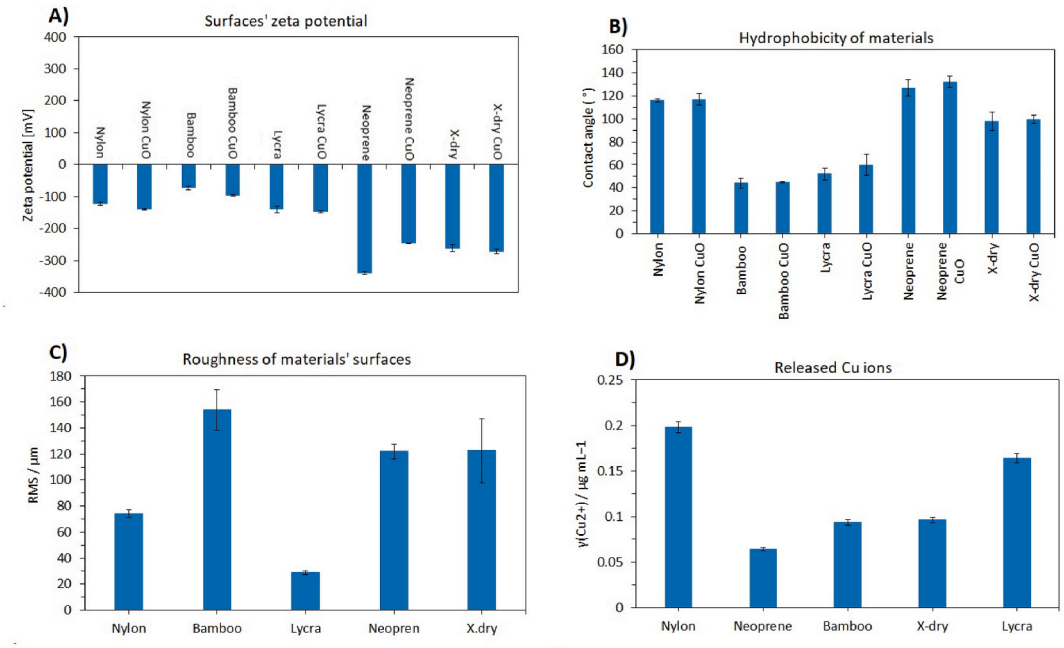

Fig. 2. Materials' surfaces characterizations. A) Zeta potential of textile material surfaces before and after CuO NPs coating; B) Water contact angle measurements on CuO NPs–coated materials. Non-treated specimens were considered control samples; C) Materials' surface roughness (root mean square – RMS) measured by optical profilometry; D) ICP-MS analysis of released copper ions from CuO NPs–coated surfaces in acetate buffer solution with pH 5.5.

exhibited slower release of the Cu ions: 0.7–1.0 μg mL^{-1} after 24 h.

3.3. Investigation of antibacterial activity

To evaluate the effect of CuO NPs–coated textile specimens against bacterial strains, a methicillin-resistant strain of *S. epidermidis* was chosen due to its pathogenic potency in skin infections. This study aimed to investigate whether the specimens coated by CuO NPs show antibacterial properties by decreasing the number of colonies and metabolic activity of attached bacteria at 24 h; metabolic activity, viability (alamar blue, CFU count) and visual analysis (SEM) have been utilized to evaluate the materials' performances. The results are represented in Fig. 3 and Table 1. As shown in Fig. 3A, metabolic activity of adhered bacteria on the surface of coated x-dry material was significantly reduced down to 60 % in comparison with both non-treated x-dry material as its control and other CuO NPs–coated specimens: neoprene, nylon, bamboo, and lycra ($p < 0.01$ indicated by **); additionally, an insignificant reduction of metabolic activity was observed when bacteria grew on the CuO NPs–coated neoprene and nylon in comparison with coated lycra and bamboo (Fig. 3A). The count of viable colonies (CFU, Table 1) detached from the materials' surfaces after 24 h indicated that the number of adhered bacteria on the CuO NPs–coated x-dry declined notably, approximately ~23 times less than the ones attached to the non-treated x-dry material (6×10^3 vs. 136×10^3 respectively), as summarized in Table 1. Visual confirmation of this result was obtained by SEM images (Fig. 3B); biofilm-like aggregates of bacteria were observed on the surface of non-treated x-dry materials, but on the coated x-dry surface, only a few colonies were detected. A slight reduction in the metabolic activity and the number of attached bacteria colonies were found on the surfaces of CuO-coated neoprene and nylon in comparison with their control materials (non-treated neoprene and nylon; Fig. 3B).

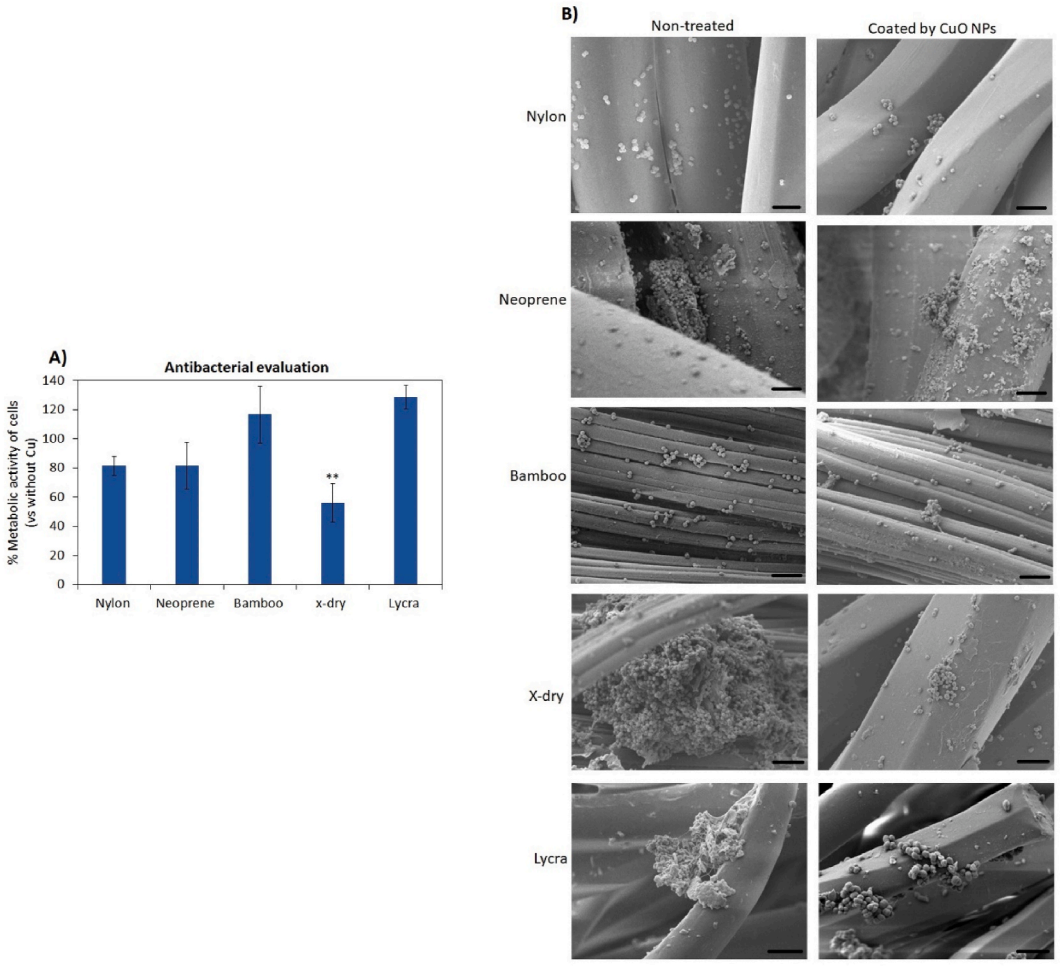

Fig. 3. Antibacterial activity evaluation. CuO NPs–coated textile specimens' surfaces were direclty infected by *S. epidermidis* after 24 h of incubation at 37 °C. A) Metabolic activity of bacterial cells; the results were normalized with non-treated specimens as control materials; B) SEM images of adhered bacterial colonies on the surface of non-treated specimens (**left panel**) and on the surface of CuO NPs–coated materials (**right panel**). (** shows pvalue <0.01, sclae bars are 5 μm).

Table 1
Counting viable bacterial cells (colony–forming unit – CFU). Surface-attached bacterial cells were counted in serial dilution 10^3 after 24 h of infection.

Materials	Adhered CFU ($\times 10^3$)				
	Nylon	Neoprene	Bamboo	X-dry	Lycra
Non-treated	3 ± 1	5 ± 1.4	250 ± 10	139 ± 18	2.5 ± 0.7
Coated by CuO NPs	1.5 ± 0.7	1.5 ± 0.7	250 ± 10	6 ± 2.8	0

3.4. Investigation of cytocompatibility activity

The direct cytocompatibility of coated specimens was investigated *in vitro* by cultivating bMSC cells on the materials' surfaces and the results represented in Fig. 4A. As shown in Fig. 4A, the metabolic activity of the attached cells onto the surfaces of bamboo, x-dry, and lycra was similar (about 75 %) and there were no statistically significant differences in comparison with the non-coated materials (as control specimens with 100 % of metabolic activity; $p > 0.05$). While, the metabolic activity of adhered cells to the surfaces of nylon and neoprene was significantly reduced to 40–50 % in comparison with control samples ($p < 0.01$ shown by **, Fig. 4A).

The potential toxic effect of the coated Cu iones on the bMSCs was evaluated by indirect assay as following the protocol ISO 10993–5: 2009. Accordingly, the coated specimens were immersed into the cell culture medium (DMEM + 10 % FBS) for 7 days. Afterwards, the culture medium including the released ions were used to cultivate cells and incubated at 37 °C for 24 h. Then, the metabolic activity of the cells and visual observation of their morphology were carried out to evaluate the effect of the released ions on the viability of the cells. As shown in Fig. 4B, the supernatant of the coated nylon and lycra significantly decreased the metabolic

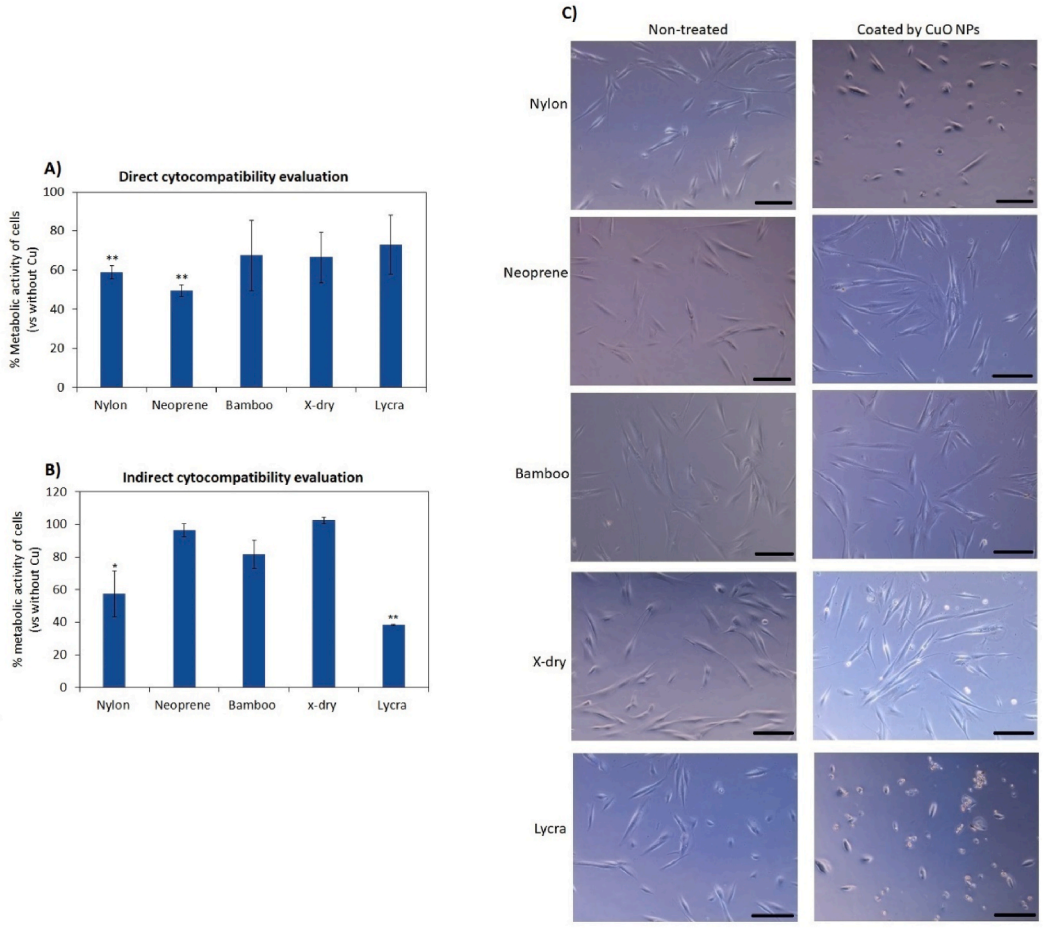

Fig. 4. Cytocompatibility evaluation on bMSC after 24 h. **Direct cytocompatibility evaluation:** A) Metabolic activity of cells directly cultivated on specimen coated by CuO NPs; the results were normalized with equivalent non–treated specimens; **Indirect cytocompatibility evaluation:** B) Metabolic activity of cells cultivated by supernatant containing released Cu ions; the results were normalized with equivalent non–treated specimens; C) Bright field microscope images of the cells after cultivation in the supernatant including released ion for 24 h (* and** show pvalue <0.05 and pvalue <0.01, respectively, scale bars = 100 μm).

activity of the cells to 70 % and 35 %, respectively, in comparison with the other coated materials (neoprene, bamboo, and x-dry; $p < 0.01$ and $p < 0.05$ indicated by ** and *, respectively). Moreover, the bright field microscope images demonstrated some detached cells (round-shaped cells) when they were cultivated with the supernatant of the coated nylone and lycra (Fig. 4C).

4. Discussion

Protection of the remaining soft tissue on the residual limb from physical and biological damages due to direct contact with prosthetic sockets or liners, such as friction, perspiration, ulceration, and bacterial infections, remains challenging. Moreover, selecting suitable materials for prosthetic liner application can notably reduce the complaints of amputees [32]. Even though there are more than 70 commercial liner products on the market, physicians select only a limited number of prosthetic liners due to a lack of knowledge about the characterization of new liners [33,34]. This study aimed to coat a wide range of textile materials (natural-based fabrics and synthetic materials) with CuO nanoparticles and evaluate their surfaces' characterization, antibacterial (against *S. epidermidis*) and cytocompatibility (bMSC) properties. To date, there is limited research on orthotic and prosthetic textiles [35], which focused on treatment with silver NPs [36] and did not consider different types of liners. Most research focuses on orthopaedic materials such as ceramics, titanium, cobalt-chromium, polymethylmethacrylate and polyethylene, which are susceptible to bacterial colonization [37]. Overall, the gathered knowledge does not cover the influence of CuO NPs on changes in the surface, cytocompatibility, and antibacterial properties of different types of materials used for prosthetic liners.

Materials' surface analyses showed no significant difference in hydrophobicity between coated specimens and non-treated ones; moreover, measurement of the static contact angle (more than 90°) for nylon, neoprene, and x-dry demonstrated that their hydrophobicity properties reduced bacterial attachment and colonization on their surface (Fig. 2B). In addition, x-dry and neoprene exhibited the most negative surface potential (Fig. 2A), which also contributes to the electrical repulsion of the negatively charged bacterial cells of *S. epidermidis* [38–40]. It has been shown that in the case of *S. epidermidis*, the high hydrophobicity of the surface and the low availability of the contact area lead to a reduction in bacterial adhesion [41]. Furthermore, our results show that prolonged exposure of *S. epidermidis* to x-dry coated with CuO NPs (Fig. 3) leads to pronounced antibacterial activity due to its slow ion release ability. Previous literature reports successful antibacterial and antiviral cotton fabric preparation by coating it with CuO NPs. Their antibacterial properties towards Gram-negative bacteria (*Escherichia coli*) revealed a zone of inhibition halo about 7 mm around the fabric [42]. Additionally, Turakhia et al. showed that even after 30 cycles of washing of CuO NPs–coated cotton fabrics, their antibacterial activity remained constant against tested Gram-positive and Gram-negative bacterial strains [43].

Finally, the cytocompatibility of the coated textile specimens was investigated *in vitro* by cultivating bMSC cells on the materials' surfaces (direct assay) and inside the supernatants containing release ions (indirect assay). In the direct assay, the metabolic activity of attached cells was reduced by 40–50 % on the CuO NPs–coated neoprene and nylon surfaces. One explanation could be that the hydrophobic properties of the nylon and neoprene surfaces (contact angles 127 and 116 for neoprene and nylon, respectively) prevented cell attachment and spread. Investigation of the toxic effect potential of Cu released from the coated specimens according to the ISO 10993–5 protocol indicated a reduction of metabolic activity down to 35 % and 70 % for lycra and nylon, respectively, after 7 days. Moreover, the bright field microscopy images demonstrated detached and rounded cells when cultivated with lycra and nylon elutes. These results confirmed the ICP-MS data showing that lycra and nylon can release Cu ions faster than other specimens and reach their concentrations up to 0.2 $\mu g\ mL^{-1}$ after 24 h. As explained in the Materials and Methods, Section 2.1.2. Textile, the materials were coated with 70 $\mu g\ mL^{-1}$ CuO NPs; furthermore, with the high rate of release of CuO NPs from the surfaces of the coated lycra and nylon, cytotoxicity levels are expected to be achieved after 7 days. From the report of Cao et al. who evaluated the cytotoxicity of different concentrations of Cu ions (0.1–100 $\mu g\ mL^{-1}$) towards L929 mouse fibroblast cells, it appears that a concentration of 40 $\mu g\ mL^{-1}$, the cells became rounded and detached from the bottom of the multiwell plate; moreover, their viability decreased down to 70 % using the MTT assay [44].

5. Conclusion

CuO NPs were synthesized and the composition of CuO was confirmed by FTIR spectroscopy and XRD analysis, whereas the SEM showed that the CuO NPs had a flake-like morphology with an irregular shape and ragged edges. The non–coated textiles exhibited negative zeta potential, different hydrophobicity, surface roughness, and structure of fiber arrangement in the material. Coating the textiles with CuO NPs did not significantly change the hydrophobicity of the materials, but it affected the zeta potential. CuO NPs–coated x-dry showed antibacterial activity towards Gram-positive pathogen *S. epidermidis*, a reduction of about 40 % in metabolic activity and about 23 times in CFU count. At the same time, no cytotoxic effect was detected on bMSC cells in direct and indirect assessments. This material seems to be a good candidate for application as a prosthetic liner and should be further investigated.

Funding

This research did not receive any specific grant from funding agencies in the public, commercial, and not-for-profit sectors.

Data availability statement

Data associated with our study has not been deposited into a publicly available repository because they are included in article/supplementary material/referenced in article.

CRediT authorship contribution statement

Ziba Najmi: Writing – review & editing, Writing – original draft, Visualization, Validation, Methodology, Investigation. **Nives Matijaković Mlinarić:** Writing – review & editing, Writing – original draft, Visualization, Validation, Methodology, Investigation, Data curation. **Alessandro Calogero Scalia:** Writing – original draft, Visualization, Validation, Methodology, Formal analysis, Data curation. **Andrea Cochis:** Writing – review & editing, Validation, Supervision, Methodology, Conceptualization. **Atiđa Selmani:** Validation, Supervision, Data curation. **Aleksander Učakar:** Validation, Supervision, Data curation. **Anže Abram:** Validation, Supervision, Data curation. **Anamarija Zore:** Validation, Supervision, Data curation. **Ida Delač:** Validation, Supervision, Data curation. **Ivan Jerman:** Validation, Supervision, Formal analysis, Data curation. **Nigel Van de Velde:** Validation, Investigation, Formal analysis, Data curation. **Janja Vidmar:** Validation, Investigation, Formal analysis, Data curation. **Klemen Bohinc:** Validation, Supervision, Funding acquisition, Data curation, Conceptualization. **Lia Rimondini:** Supervision, Project administration, Funding acquisition, Data curation, Conceptualization.

Declaration of competing interest

The authors declare that they have no known competing financial interests or personal relationships that could have appeared to influence the work reported in this paper.

Acknowledgements

N.M.M. thank ARRS for support through the project « Antibacterial and antiviral properties of nano-coated surfaces», N1-0264. A.S. would like to thank Anton Paar Croatia d. o.o. Zagreb, Croatia, for providing the instrument Litesizer 500 for use and analysis. I.D. acknowledges financial support of the Center of Excellence for Advanced Materials and Sensing Devices, ERDF (European Regional Develompent Fund) Grant No. KK.01.1.January 1, 0001.

The authors thank Moor Ortotika Protetika d. o.o. For delivering materials.

Appendix A. Supplementary data

Supplementary data to this article can be found online at https://doi.org/10.1016/j.heliyon.2023.e23849.

References

[1] T.S. Lim, A. Finlayson, J.M. Thorpe, K. Sieunarine, B.P. Mwipatayi, A. Brady, M. Abbas, D. Angel, Outcomes of a contemporary amputation series, ANZ J. Surg. 76 (2006) 300–305, https://doi.org/10.1111/j.1445-2197.2006.03715.x.

[2] C.L. McDonald, S. Westcott-McCoy, M.R. Weaver, J. Haagsma, D. Kartin, Global prevalence of traumatic non-fatal limb amputation, Prosthet. Orthot. Int. 45 (2021) 105–114, https://doi.org/10.1177/0309364620972258.

[3] G.K. Klute, B.C. Glaister, J.S. Berge, Prosthetic liners for lower limb amputees, Prosthet. Orthot. Int. 34 (2010) 146–153, https://doi.org/10.3109/03093641003645528.

[4] I. Boudjemaa, A. Sahli, A. Benkhettou, S. Benbarek, Effect of multi-layer prosthetic foam liner on the stresses at the stump–prosthetic interface, Frat. Ed. Integrità Strutt. 15 (2021) 187–194, https://doi.org/10.3221/IGF-ESIS.56.15.

[5] S.P. Miguel, R.S. Sequeira, A.F. Moreira, C.S.D. Cabral, A.G. Mendonça, P. Ferreira, I.J. Correia, An overview of electrospun membranes loaded with bioactive molecules for improving the wound healing process, Eur. J. Pharm. Biopharm. 139 (2019) 1–22, https://doi.org/10.1016/j.ejpb.2019.03.010.

[6] E.A. Grice, J.A. Segre, The skin microbiome, Nat. Rev. Microbiol. 9 (2011) 244–253, https://doi.org/10.1038/nrmicro2537.

[7] Z. Qiao, S. Huang, F. Leng, Y. Bei, Y. Chen, M. Chen, Y. Hu, Y. Huang, Q. Xiang, Analysis of the bacterial flora of sensitive facial skin among women in guangzhou, Clin. Cosmet. Invest. Dermatol. 14 (2021) 655–664, https://doi.org/10.2147/CCID.S307668.

[8] J.M. Haglin, D.R. Garcia, D.L. Roque, C.S.L. Spake, J.D. Jarrell, C.T. Born, Assessing the efficacy of a silver carboxylate antimicrobial coating on prosthetic liners, Journal of Prosthetics and Orthotics 32 (2020) 251–257, https://doi.org/10.1097/JPO.0000000000000271.

[9] C. Quintero-Quiroz, L.E. Botero, D. Zárate-Triviño, N. Acevedo-Yepes, J.S. Escobar, V.Z. Pérez, L.J. Cruz Riano, Synthesis and characterization of a silver nanoparticle-containing polymer composite with antimicrobial abilities for application in prosthetic and orthotic devices, Biomater. Res. 24 (2020) 13, https://doi.org/10.1186/s40824-020-00191-6.

[10] M.E. Stryjewski, H.F. Chambers, Skin and soft-tissue infections caused by community-acquired methicillin-resistant *Staphylococcus aureus*, Clin. Infect. Dis. 46 (2008) S368, https://doi.org/10.1086/533593. –S377.

[11] X. Yang, R. Zhao, D. Solav, X. Yang, D.R.C. Lee, B. Sparrman, Y. Fan, H. Herr, Material, design, and fabrication of custom prosthetic liners for lower-extremity amputees: a review, Med Nov Technol Devices 17 (2023), 100197, https://doi.org/10.1016/j.medntd.2022.100197.

[12] M.S. Wong, B. Hassan Beygi, Y. Zheng, Materials for exoskeletal orthotic and prosthetic systems, in: Encyclopedia of Biomedical Engineering, Elsevier, 2019, pp. 352–367, https://doi.org/10.1016/B978-0-12-801238-3.11040-2.

[13] R.Y. Pelgrift, A.J. Friedman, Nanotechnology as a therapeutic tool to combat microbial resistance, Adv. Drug Deliv. Rev. 65 (2013) 1803–1815, https://doi.org/10.1016/j.addr.2013.07.011.

[14] Z. Ni, X. Gu, Y. He, Z. Wang, X. Zou, Y. Zhao, L. Sun, Synthesis of silver nanoparticle-decorated hydroxyapatite (HA@Ag) poriferous nanocomposites and the study of their antibacterial activities, RSC Adv. 8 (2018) 41722–41730, https://doi.org/10.1039/C8RA08148D.

[15] Y. Wu, Y. Yang, Z. Zhang, Z. Wang, Y. Zhao, L. Sun, Fabrication of cotton fabrics with durable antibacterial activities finishing by Ag nanoparticles, Textil. Res. J. 89 (2019) 867–880, https://doi.org/10.1177/0040517518758002.

[16] S.V. Gudkov, D.E. Burmistrov, D.A. Serov, M.B. Rebezov, A.A. Semenova, A.B. Lisitsyn, A mini review of antibacterial properties of ZnO nanoparticles, Front. Physiol. 9 (2021), https://doi.org/10.3389/fphy.2021.641481.

[17] C. Kaweeteerawat, C.H. Chang, K.R. Roy, R. Liu, R. Li, D. Toso, H. Fischer, A. Ivask, Z. Ji, J.I. Zink, Z.H. Zhou, G.F. Chanfreau, D. Telesca, Y. Cohen, P.A. Holden, A.E. Nel, H.A. Godwin, Cu nanoparticles have different impacts in Escherichia coli and lactobacillus brevis than their microsized and ionic analogues, ACS Nano 9 (2015) 7215–7225, https://doi.org/10.1021/acsnano.5b02021.

[18] Y.-H. Hsueh, P.-H. Tsai, K.-S. Lin, pH-Dependent antimicrobial properties of copper oxide nanoparticles in Staphylococcus aureus, Int. J. Mol. Sci. 18 (2017) 793, https://doi.org/10.3390/ijms18040793.
[19] R.G. Chaudhary, V.N. Sonkusare, G.S. Bhusari, A. Mondal, D.P. Shaik, H.D. Juneja, Microwave-mediated synthesis of spinel CuAl2O4 nanocomposites for enhanced electrochemical and catalytic performance, Res. Chem. Intermed. 44 (2018) 2039–2060, https://doi.org/10.1007/s11164-017-3213-z.
[20] V. Stanić, S.B. Tanasković, Antibacterial activity of metal oxide nanoparticles, in: Nanotoxicity, Elsevier, 2020, pp. 241–274, https://doi.org/10.1016/B978-0-12-819943-5.00011-7.
[21] L.E. Román, E.D. Gomez, J.L. Solís, M.M. Gómez, Antibacterial cotton fabric functionalized with copper oxide nanoparticles, Molecules 25 (2020) 5802, https://doi.org/10.3390/molecules25245802.
[22] S. Shahidi, A. Jamali, S. Dalal Sharifi, H. Ghomi, In-situ synthesis of CuO nanoparticles on cotton fabrics using spark discharge method to fabricate antibacterial textile, J. Nat. Fibers 15 (2018) 870–881, https://doi.org/10.1080/15440478.2017.1376302.
[23] Z. Ni, M. Wan, G. Tang, L. Sun, Synthesis of CuO and PAA-regulated silver-carried CuO nanosheet composites and their antibacterial properties, Polymers 14 (2022) 5422, https://doi.org/10.3390/polym14245422.
[24] A. Abram, A. Zore, U. Lipovž, A. Košak, M. Gavras, Ž. Boltežar, K. Bohinc, Bacterial adhesion on prosthetic and orthotic, Material Surfaces, Coatings 11 (2021) 1469, https://doi.org/10.3390/coatings11121469.
[25] K. Bohinc, R. Štukelj, A. Abram, I. Jerman, N. Van de Velde, R. Vidrih, Biophysical characterization of autochthonous and new apple cultivar surfaces, Agronomy 12 (2022), https://doi.org/10.3390/agronomy12092051.
[26] J.J. Harrison, C.A. Stremick, R.J. Turner, N.D. Allan, M.E. Olson, H. Ceri, Microtiter susceptibility testing of microbes growing on peg lids: a miniaturized biofilm model for high-throughput screening, Nat. Protoc. 5 (2010) 1236–1254, https://doi.org/10.1038/nprot.2010.71.
[27] E. Jablonská, J. Kubásek, D. Vojtěch, T. Ruml, J. Lipov, Test conditions can significantly affect the results of in vitro cytotoxicity testing of degradable metallic biomaterials, Sci. Rep. 11 (2021) 6628, https://doi.org/10.1038/s41598-021-85019-6.
[28] G.K. Srivastava, M.L. Alonso-Alonso, I. Fernandez-Bueno, M.T. Garcia-Gutierrez, F. Rull, J. Medina, R.M. Coco, J.C. Pastor, Comparison between direct contact and extract exposure methods for PFO cytotoxicity evaluation, Sci. Rep. 8 (2018) 1425, https://doi.org/10.1038/s41598-018-19428-5.
[29] H. Siddiqui, M.S. Qureshi, F.Z. Haque, Valuation of copper oxide (CuO) nanoflakes for its suitability as an absorbing material in solar cells fabrication, Optik 127 (2016) 3713–3717, https://doi.org/10.1016/j.ijleo.2015.12.133.
[30] K.J. Arun, A.K. Batra, A. Krishna, K. Bhat, M.D. Aggarwal, P.J. Joseph Francis, Surfactant free hydrothermal synthesis of copper oxide nanoparticles, Am. J. Mater. Sci. 5 (2015) 36–38, https://doi.org/10.5923/s.materials.201502.06.
[31] D. Kovačević, R. Pratnekar, K.G. Torkar, J. Salopek, G. Dražić, A. Abram, K. Bohinc, Influence of polyelectrolyte multilayer properties on bacterial adhesion capacity, Polymers 8 (2016) 345–357, https://doi.org/10.3390/polym8100345.
[32] B.A. Pascale, B.K. Potter, Residual limb complications and management strategies, Curr Phys Med Rehabil Rep 2 (2014) 241–249, https://doi.org/10.1007/s40141-014-0063-0.
[33] J.C. Cagle, B.J. Hafner, N. Taflin, J.E. Sanders, Characterization of prosthetic liner products for people with transtibial amputation, JPO J. Prosthetics Orthot. 30 (2018) 187–199, https://doi.org/10.1097/JPO.0000000000000205.
[34] B.J. Hafner, J.C. Cagle, K.J. Allyn, J.E. Sanders, Elastomeric liners for people with transtibial amputation, Prosthet. Orthot. Int. 41 (2017) 149–156, https://doi.org/10.1177/0309364616661256.
[35] A. Rohani Shirvan, A. Nouri, Medical textiles, in: Advances in Functional and Protective Textiles, Elsevier, 2020, pp. 291–333, https://doi.org/10.1016/B978-0-12-820257-9.00013-8.
[36] U. Klueh, V. Wagner, S. Kelly, A. Johnson, J.D. Bryers, Efficacy of silver-coated fabric to prevent bacterial colonization and subsequent device-based biofilm formation, J. Biomed. Mater. Res. 53 (2000) 621–631, https://doi.org/10.1002/1097-4636(2000)53:6<621::AID-JBM2>3.0.CO;2-Q.
[37] D.J. Davidson, D. Spratt, A.D. Liddle, Implant materials and prosthetic joint infection: the battle with the biofilm, EFORT Open Rev 4 (2019) 633–639, https://doi.org/10.1302/2058-5241.4.180095.
[38] K.C. Marshall, R. Stout, R. Mitchell, Mechanism of the initial events in the sorption of marine bacteria to surfaces, J. Gen. Microbiol. 68 (1971) 337–348, https://doi.org/10.1099/00221287-68-3-337.
[39] H.H.M. Rijnaarts, W. Norde, J. Lyklema, A.J.B. Zehnder, DLVO and steric contributions to bacterial deposition in media of different ionic strengths, Colloids Surf. B Biointerfaces 14 (1999) 179–195, https://doi.org/10.1016/S0927-7765(99)00035-1.
[40] A.T. Poortinga, R. Bos, W. Norde, H.J. Busscher, Electric double layer interactions in bacterial adhesion to surfaces, Surf. Sci. Rep. 47 (2002) 1–32, https://doi.org/10.1016/S0167-5729(02)00032-8.
[41] L.C. Xu, C.A. Siedlecki, Staphylococcus epidermidis adhesion on hydrophobic and hydrophilic textured biomaterial surfaces, Biomed. Mater. (2014) 9, https://doi.org/10.1088/1748-6041/9/3/035003.
[42] F.S. Hussain, N. Memon, Z. Khatri, Facile process for the development of antiviral cotton fabrics with nano-embossed copper oxide, ACS Omega 8 (2023) 18617–18625, https://doi.org/10.1021/acsomega.3c00492.
[43] B. Turakhia, M.B. Divakara, M.S. Santosh, S. Shah, Green synthesis of copper oxide nanoparticles: a promising approach in the development of antibacterial textiles, J. Coating Technol. Res. 17 (2020) 531–540, https://doi.org/10.1007/s11998-019-00303-5.
[44] B. Cao, Y. Zheng, T. Xi, C. Zhang, W. Song, K. Burugapalli, H. Yang, Y. Ma, Concentration-dependent cytotoxicity of copper ions on mouse fibroblasts in vitro: effects of copper ion release from TCu380A vs TCu220C intra-uterine devices, Biomed. Microdevices 14 (2012) 709–720, https://doi.org/10.1007/s10544-012-9651-x.